Ca alleviated Cd-induced toxicity in Salix matsudana by affecting Cd absorption, translocation, subcellular distribution, and chemical forms

Xiaoshuo Shang
Tianjin Normal University
Wenxiu Xue
Tianjin Normal University
Yi Jiang
Tianjin Normal University
Jinhua Zou (zjhmon@126.com)
Tianjin Normal University https://orcid.org/0000-0002-2740-4967

Research article

Keywords: Cd, Ca, S. matsudana, Cd uptake and translocation, subcellular distribution, chemical forms, energy dispersive X-ray analyses (EDXA).

Posted Date: February 26th, 2020

DOI: https://doi.org/10.21203/rs.2.24734/v1

Abstract

Background: Cadmium (Cd), a ubiquitous and highly toxic heavy metal pollutant, is toxic to animals and plants. Calcium (Ca) is an essential component for plant growth and reduces plant Cd adsorption by competing with Cd. To gain deeper insight into the effects of Ca on Cd absorption, translocation, subcellular distribution, and chemical forms in S. matsudana seedlings under Cd stress, an investigation was conducted on these properties. Results: Adding Ca alleviated Cd physiological toxicity in S. matsudana, reduced Cd adsorption, increased the translocation from roots to shoots, lead to subcellular redistribution of Cd by increasing the proportion of Cd in soluble fractions but decreasing Cd in the cell wall and changed the chemical forms of Cd from 0.6 M HCl- and 2% HAc-extracted Cd to 1 M NaCl-extracted Cd. The energy dispersive X-ray analyses (EDXA) results revealed that after adding Ca, Cd was transferred through the root epidermis, cortex, endodermis, and vascular cylinder, transported to the shoots, and was highly accumulated in leaf epidermal and mesophyll cells, but less in leaf vein and guard cells. The genes involved in Cd uptake and xylem loading included NRAMP1, ZIP8, HMA2, and HMA4, which were up-regulated significantly ($p < 0.05$) in the Cd and Cd + Ca treatments compared to the control. Conclusions: The findings of this study provide new insight into the mechanism that Ca alleviates Cd toxicity in woody tree species, as well as propose an important prospect of Ca addition for improving the phytoremediation of Cd contamination.

Background

Cadmium (Cd) is a ubiquitous and highly toxic heavy metal pollutant that is toxic to animals and plants [1]. Considerable attention has focused on the problems associated with Cd pollution as modern industries and agriculture have developed. Plant Cd accumulation and the subsequent trophic transfer in the food chain pose a serious threat to ecosystems and human health [2, 3]. Cd affects the growth and development of plants, inhibits photosynthesis and respiration, imbalances water and nutrient absorption [4–7], and ultimately results in reduced biomass, leading to leaf yellowing, inhibited root growth and even plant death [8–10]. Therefore, it is of great importance to better our understanding of the Cd toxicity mechanism in plants [11, 12].

Calcium (Ca) is essential for plant growth and reduces plant Cd adsorption by competing with Cd [13, 14]. Ca is fundamentally important for membrane permeability and maintaining cell integrity and ion uptake, which allows solute diffusion in plant tissues [15]. Ca is an essential component in signal transduction pathways under abiotic and biotic stress, and small intracellular changes in free Ca concentration regulate certain processes, such as cell elongation and division [16].

Ca and Cd are both divalent metals that have similar chemical properties. Both can enter cells through different channels or through protein-dependent permeation [17]. Some evidence suggests that Ca may raise the tolerance to Cd and minimize the damage induced by Cd in plants [18, 19]. Hayakwa et al. [20] indicated that Ca could inhibit Cd transport from the roots to stems and leaves. In a previous investigation, 5 mM Ca alleviated the toxic effects of Cd on *S. matsudana* seedling growth and promoted

the uptake of copper (Cu), iron (Fe), zinc (Zn), and manganese (Mn) to different degrees [7]. However, the Ca mechanism that affects Cd accumulation in plants remains to be clarified, especially in Cd subcellular localization and chemical forms modification of plant cells under Cd stress.

Previous studies demonstrated that heavy metal subcellular localization, chemical forms and their mobility may be related to heavy metal detoxification and tolerance in plants [21–25]. Previous investigations also indicated that the stored forms of Cd in plant cells affect Cd uptake, accumulation and tolerance [25, 26]. Moreover, some evidence suggests that NaCl-extractable Cd in plants play an important role in the minimization of Cd toxicity [27, 28]. After Cd is absorbed by plant roots and leaves, Cd is distributed in various tissues, which can be got by energy-dispersive X-ray analyses (EDXA) [29–31]. However, only a few studies on the effects of Ca on Cd subcellular distribution and its chemical forms in plants under Cd stress have been reported.

It was reported that Cd could inhibit the photosynthetic process, including chlorophyll biosynthesis, the assembly of pigment protein complexes and thylakoids, the electron transport chain, Calvin cycle enzymes activity, and sugar transport and consumption [32]. Some studies on photosynthetic responses in plants under Cd stress have been reported [33]. However, only a few studies have reported on the effects of Ca on chlorophyll fluorescence and photosynthesis parameters in woody plants under Cd stress.

Cd has no specific transporter and is absorbed, transported, and distributed mainly by various transporters through synergistic actions in plants [34, 35]. These transporters include cation diffusion facility (CDF) proteins, heavy metal ATPases (HMA) of the P1B-type ATPase, natural resistance-associated macrophage proteins (NRAMP), and zinc-regulated transporters and iron-regulated transporter-like proteins (ZIP) [36]. CDF is responsible for the transfer of metal ions from the intracellular to extracellular space, HMA is responsible for metal ion transport through the energy released by ATP hydrolysis, NRAMP is involved in the transport of divalent metal cations, and ZIP is involved in the process of metal ion absorption, transport, and distribution.

Chinese willow trees (*Salix matsudana* Koidz) are widely cultivated in China, which adapt to broad range of climatic conditions [25]. It is one of the most important landscaping and timber tree species and is characterized by its easy reproduction and cultivation, large biomass, rapid growth, deep root system, and tolerance of high transpiration to hypoxic conditions [29, 37]. Thus, *S. matsudana* has great potential in repairing of Cd contaminated soils and water [25, 38, 39].

In order to gain deeper insight into how Ca alleviates Cd-induced toxicity and affects this process during Cd uptake, an investigation on Cd translocation, redistribution, and chemical forms in *S. matsudana* seedlings under Cd stress was conducted in this study.

Results

Ca effects on *S. matsudana* physiology under Cd stress

Control plants grew well, the branches were lush, and the leaves were bright green. In the Cd treatment groups, there were fewer branches, and the leaves had yellowed. The branches of the 50 μM Cd treatment group were sparse, the leaves were narrow and small even appeared yellow. After the addition of 5 mM Ca, the Cd toxicity to *S. matsudana* was obviously alleviated (Fig. 1).

Changes in the photosynthetic fluorescence parameters of *S. matsudana* treated with different Cd and Cd + Ca concentrations for 28 d are presented (Table 1). Compared to the control, the minimum (dark) fluorescence($F_{0)}$, the maximum fluorescence($F_{m)}$, the maximum efficiency of PSII photochemistry in the dark-adapted state($F_v/F_{m)}$, the quantum yield of PSII electron transport(YII), and the photochemical quenching coefficient(qP) decreased significantly ($p < 0.05$) after Cd treatment, while the non-photochemical quenching coefficient(qN) increased significantly ($p < 0.05$), indicating that photosynthesis under Cd stress was inhibited. However, the results also revealed that the addition of Ca inhibited the decrease of F_0, F_m, F_v/F_m, YII, and qP and increase of qN, indicating that Ca played a positive role in this process.

Cd uptake and translocation

The data of Table 2 demonstrated that Cd content of different *S. matsudana* organs varied among all Cd and Cd + Ca treatments. Comparing with the control, the root Cd concentrations in 10 and 50 μM Cd-treated plants raised obviously ($p < 0.05$). The Cd contents of other organs also increased as Cd concentrations increased. The Cd levels in different organs were ordered as follows after 28 d of treatment: roots > new stems > leaves > old stems. The data indicated that Ca addition decreased Cd contents of all the organs significantly ($p < 0.05$). Moreover, the addition of Ca increased the Cd translocation factor (TF) when compared to treatments with Cd alone, although adding Ca decreased the Cd content of the whole plant (Table 2).

Cd was actively absorbed and translocated through the transporters, NRAMP1, ZIP8, HMA2, and HMA4, under Cd stress, and their expressions increased significantly ($p < 0.05$), while IRT1 expression decreased when contrasted with the control (Fig. 2). In the Cd + Ca treatment group, the expression levels of NRAMP1, ZIP8, HMA2, and HMA4 maintained high levels when compared to the control plants but decreased significantly ($p < 0.05$) when compared to the Cd treatment group. PCR1 took part in Ca radial transportation in the roots and its upward translocation. Compared to the control and Cd treatment group, the expression of PCR1 in the Cd + Ca treatment group increased significantly ($p < 0.05$)(Fig. 2B). These results suggested that Ca plays an important role in aboveground plant parts.

Cd subcellular distribution

The EDXA data uncovered the Cd subcellular distribution in the mature zone of root tip cells treated with 50 μM Cd and 50 μM Cd + 5 mM Ca after 24 h (Fig. 3). The Cd contents in the three root tip zones of mature zone cells exposed to Cd differed and were ordered as follows: vascular cylinder (1.56 wt%) > cortex (1.34 wt%) > epidermis (0.55 wt%). After the addition of 5 mM Ca, the Cd contents of the three root

tip zones of mature zone cells were ordered as follows: vascular cylinder (1.33 wt%) > cortex (1.18 wt%) > epidermis (0.45 wt%).

The EDXA data also uncovered the subcellular localization of Cd in the leaves exposed to 50 μM Cd and 50 μM Cd + 5 mM Ca after 28 d (Fig. 4). The Cd contents in the three zones of the leaves exposed to Cd differed and were ordered as follows: leaf epidermal cells (1.05 wt%) > leaf main vein (0.69 wt%) > leaf epidermal stomata (0.40 wt%). After the addition of 5 mM Ca, the Cd contents of the three leaf zones were ordered as follows: leaf epidermal cells (0.88 wt%) > leaf main veins (0.58 wt%) > leaf epidermal stomata (0.34 wt%). Collectively, these results suggested that Cd was mainly distributed in leaf epidermal and mesophyll cells in the Cd and Cd + Ca treatment groups.

The Cd subcellular deposition was shown as the Cd content in different subcellular fractions (i.e., cell wall, cell organelles, and soluble fractions) in *S. matsudana* roots and leaves (Table 3, Fig. 5). Results indicated that the majority of Cd was located in the cell wall and soluble fractions. The Cd contents of all three subcellular components increased significantly ($p < 0.05$) as Cd concentration increased. The proportion of Cd among the three fractions in the leaves was ordered as follows: soluble fractions > cell wall > cell organelles. In roots, the order was as follows: cell wall > soluble factions > cell organelles. The application of Ca resulted in the subcellular redistribution of Cd in *S. matsudana*. In both the roots and leaves, Ca addition increased the proportion of Cd in soluble fractions but decreased the proportion of Cd in the cell wall when compared to treatments with Cd alone.

Cd chemical forms

The diverse chemical forms of Cd in *S. matsudana* roots and leaves exposed to all Cd and Cd + Ca treatments after 28 d were extracted and determined with different extracting solutions. The Cd contents and percentages of the chemical forms are presented (Table 4, Fig. 6). The Cd contents with different chemical forms raised obviously ($p < 0.05$) as Cd concentrations increased. The percentage of different chemical forms varied with Cd and Ca concentrations (Fig. 6). Results revealed that 1 M NaCl and 2% HAc extracted the highest Cd content in all the Cd treatments. The proportion of Cd chemical forms in the leaves and roots were ordered as follows: $Cd_{NaCl} > Cd_{HAc} > Cd_{HCl} > Cd_W > Cd_E > Cd_R$. Moreover, in the roots and leaves, the proportion of Cd extracted with 1 M NaCl decreased as the Cd concentration increased from 10 to 50 μM, while the proportion of Cd extracted using 2% HAc and 0.6 M HCl increased (Fig. 6).

The results also revealed that the addition of Ca decreased the contents of distrinct Cd chemical forms in both roots and leaves when contrasted with treatments with Cd alone (Fig. 6). The addition of Ca altered the proportion of different Cd chemical forms in *S. matsudana* by means of elevating the percentage of 1 M NaCl-extracted Cd and lowering the proportion of 0.6 M HCl- and 2% HAc-extracted Cd in the leaves and roots.

Discussion

Ca addition alleviated Cd physiological toxicity

Cd stress induces alterations in photosynthetic rates, photosynthetic pigments, chlorophyll fluorescence, and nutrient homeostasis [39, 40]. Photosynthesis is especially sensitive to Cd. The chlorosis of leaves is one of the first visible symptoms of Cd toxicity, which is due to decreased rates of chlorophyll biosynthesis and chlorophyll contents caused by damage to thylakoid membranes [33]. In this study, chlorosis symptoms in *S. matsudana* leaves exposed to different Cd concentrations were observed. This phenomenon was more obvious as Cd concentrations increased. The addition of Ca effectively alleviated Cd toxicity in Cd-treated plants. A previous study indicated a internal mechanism for depressing the Cd toxicity as Ca concentrations increased in plant roots exposed to Cd, that when both Cd and Ca exist in the soil system, Ca and Cd exhibit similar chemical properties, Ca competes with Cd at adsorption sites in the soil, as a result, Cd uptake is reduced by Ca, then reducing Cd toxic effects in plants [7, 13, 20, 23].

Chlorophyll fluorescence is an effective measure of photosynthesis in light reactions. F_v/F_m and Y(II) are representative fluorescence parameters that are widely used to evaluate the effects of environmental stress on plants [41]. Chlorophyll fluorescence depends, to a great extent, on pigment contents and the capability of leaves to photosynthesize. In this study, the effects of Ca on Cd-induced damage in *S. matsudana* were investigated. The chlorophyll fluorescence parameters, F_0, F_m, F_v/F_m, Y(II), and qP, significantly decreased and qN increased in *S. matsudana* after treatment with 50 μM Cd. Moreover, changes in these parameters revealed the damage of Cd toxicity to the photosynthetic apparatus. Cd disturbed the photosynthesis reaction center and restrained this process [33]. Ge et al. [33] also indicated that Cd reduced Fe contents, which resulted in decreased chlorophyll contents in *Populus* leaves. This study demonstrated that the addition of exogenous Ca inhibited the decrease of F_0, F_m, F_v/F_m, YII, and qP and the increase of qN, indicating that Ca played a positive role in this process. He et al. [42] found that exogenous Ca enhanced the electron transport capacity of cucumbers and reduced stress-induced damage. Moreover, exogenous Ca application increased the net photosynthesis rate, stomatal conductance, intercellular CO_2 concentration, and maximum quantum efficiency of photosystem II photochemistry, YII, and qP [43].

Ca addition changed Cd uptake and translocation

EDXA is an analytical technique used for analyzing the elemental subcellular localization in biological specimens[31, 44]. The results by scanning electron microscope (SEM) and EDXA revealed that the Cd contents of root epidermis, cortex, and vascular cylinder cells in Cd-treated roots were lower than those in Cd + Ca-treated roots. Moreover, Cd absorbed in the roots passed through the root epidermis, cortex, and endodermis and was transported to the shoots in Cd and Cd + Ca-treated *S. matsudana* (Fig. 3). The Cd adsorption through the symplastic pathway was depressed in Cd + Ca-treated plants but enhanced in Ca-treated plants. However, the exact role that Ca addition plays in Cd uptake and transportation still remains unclear as no specific Cd transporter was ascertained in previous studies. Thus, Cd may be absorbed by metal transporters or through a similar mechanism, such as ZIP, NRAMP, or HMA. It was reported that the AtZIP2 and AtZIP4 expression levels correlated with Cd concentrations positively in Cd-treated plants,

indicating that the Cd absorption by AtZIP2 and AtZIP4 depended on Cd concentrations, but after Ca application, their expression levels decreased obviously [45]. Similar results in the expression levels of NRAMP1 and ZIP8 in *S. matsudana* were observed in this study (Fig. 2A). SmNRAMP1 and SmZIP8, which are involved in Cd absorption and transportation, exhibited higher expression levels in Cd-treated plants than Cd + Ca-treated plants. The investigations of Nakanishi et al. may explained the subtle changes in the expression level of IRT1 [46]. It was concluded that Ca reduced Cd adsorption because adding Ca changed Cd transport process. Notably, the gene expression results uncovered an important fact that may lead to Cd uptake differences in various treatments of this study.

In previous studies, the addition of Ca decreased the amount of Cd in whole plants, including *Arabidopsis thaliana* [45], *Zea mays* [47], *Trifolium repens* [48], *Brassica napus* [49], *Lens culinaris* [50], *Matricaria chamomilla* [51], and *Boehmeria nivea* [52]. Similar results were obtained in this study. The Cd contents in Cd + Ca-treated plants were significantly lower when compared to treatments with Cd alone, regardless of the dose (Table 2). Moreover, the TF of Cd in Cd + Ca-treated plants was higher than that in Cd- treated alone. Additionally, the changes in SmHMA2 and SmHMA4 expression levels in this study were induced by the Cd and Cd + Ca treatments (Fig. 2B), which confirmed that HMA2 and HMA4 participated in the upward-translocation of Cd. Similarly, the effluxion of Zn and Cd was resulted in by overexpression of HMA4 in yeast and *E. coli*, indicating that HMA4 played an important role in Cd xylem uploading [53, 54]. It was further noted that adding Ca promoted the xylem-loading and upward transportation of Cd based on the expression levels of related gene.

The radial translocation of Ca from the roots to shoots was promoted by the *B. juncea* plant cadmium resistance 1 (BjPCR1) protein, the transportation of Ca to the shoots was disturbed and the plant growth was inhibited by knock-out of BjPCR1[55, 56]. The expression levels of SmPCR1 was up-regulated in this study suggested that it play a major role in Ca adsorption and transportation. It was reported that Ca accumulate mainly in the epidermal cells and trichomes, which played an important role in some accumulative plant species, which was dependent on the plant species [57].

Ca addition induced Cd subcellular redistribution

The results of Fig. 4 revealed that Cd accumulated mainly in leaf epidermal and mesophyll cells, which was greater than in leaf main veins or guard cells. These results suggested that the leaf epidermal and mesophyll cells were the main site of Cd. Huguet et al. [58] also found that in leaves Cd accumulated mainly in leaf edges, and less concentrated in regions around leaf vascular bundles. Leitenmaier and Kupper [59] also reported that the Cd uptake rate in epidermal storage cells was greater than in epidermal or mesophyll cells. Shi et al. [30] observed high Cd levels in the epidermis, veins, and stomata near necrotic spots on leaves exposed to Cd. Cd accumulation and cell death have obvious relevance with the leaves exposed to Cd. After the addition of Ca, the Cd contents in the 3 leaf regions all decreased, and the proportion of Cd in leaf epidermal cells significantly increased, indicating that Ca application led to the redistribution of Cd in *S. matsudana* leaves. Based on these findings, it was assumed that the reduction

of Cd toxicity in the leaves may have resulted from the Ca regulation of Cd contents in leaf epidermis cells. However, further investigations are required to verify these results.

The Cd contents of different subcellular fractions have extremely important influences on Cd uptake, translocation, distribution and detoxification in different plant species [60–62]. The data of this study demonstrated that Cd (86.7%–97.7%) in *S. matsudana* leaf and root cells was stored in the cell wall and soluble fractions. Cd (66%–77%) in *S. matsudana* roots was stored in the cell wall, while a small quantity of Cd was located in organelle fractions. However, in *S. matsudana* leaves, Cd (45%–55%) was found in soluble fractions. These results are the same as the findings of Huang et al. [21] and Lu et al. [23]. Moreover, Wu et al. [25] also indicated that Cd was located in the cell wall of *S. matsudana* roots after treatment with 50 μM Cd. The cell wall is the first protective barrier that protects the protoplast from Cd toxicity and mainly comprised polyose and proteins, which can bind Cd ions on their surfaces and limit Cd migration across the cell membrane [21, 23, 60]. When Cd ions enter the cytosol, it is chelated by phytochelatin to form metal complexes in order to minimize Cd stress [25, 63, 64]. Wang et al. [65] found that most Cd in the cytosol was transformed into less toxic chemical forms and translocated into the vacuole, thereby minimizing Cd toxicity. Ma et al. [66] also reported that the internal detoxification of Cd and Zn in *Thlaspi caerulescens* leaves was achieved by vacuolar compartmentalization.

In this investigation, the application of Ca altered Cd subcellular distribution in *S. matsudana*, uncovering an important process of Ca alleviating Cd stress in plants (Fig. 5). After the addition of Ca, the percentage of Cd in the cell walls of *S. matsudana* roots and leaves decreased, while the percentage of Cd in soluble fractions increased. These results suggested that *S. matsudana* avoided Cd stress by chelating the free Cd in the protoplasm to form metal complexes, thereby fixing Cd in the vacuole through compartmentalization. Similarly, Choi et al. [67] found that seedlings treated with Cd in the presence of Ca exhibited increased tolerance, which was proportional to increases in Ca concentrations.

Ca addition modified Cd chemical forms

The chemical form of Cd in plants is very important and reflects the degree of Cd migration and toxicity. Different Cd chemical forms are connected with various Cd biological activities in plants [64]. Cd in inorganic forms (Cd_W) and organic forms (Cd_E) are more mobile than other chemical forms, and more toxic to plant cells. Pectate- and protein-integrated Cd (Cd_{NaCl}), insoluble Cd phosphate (Cd_{HAc}), and Cd oxalate (Cd_{HCl}), are less mobile and less toxic to plant cells [60, 68–70]. In this study, Cd concentrations of different chemical forms in *S. matsudana* roots and leaves increased as Cd concentrations increased (Fig. 6). Cd extracted with 1 M NaCl and 2% HAc was the predominant chemical form in *S. matsudana* roots and leaves, while Cd extracted with other extracting solutions was rather low (Fig. 6). These results are consistent with earlier findings [25, 64, 71, 72, 73]. Wu et al. [25] demonstrated that NaCl extractants combine to pectic acids and proteins to which Cd was fixed. In *S. matsudana* roots and leaves, the proportion 1 M NaCl-extracted Cd decreased, while the proportion of 0.6 M HCl- and 2% HAc-extracted Cd increased as Cd concentrations increased from 10 to 50 μM (Fig. 6). The results suggested that, as Cd concentrations increased, Cd may have transformed into inactive metal complexes to protect the cells. Li

et al. [74] also demonstrated that converting Cd into non-toxic pectate- and protein-bound forms could minimize the Cd toxicity. Qiu et al. drew the same conclusion that the Cd in pectate- and protein-chelated forms was correlated with Cd bound to cell wall fractions in *B. parachinensis* [75], then limited Cd translocation from roots to shoots [26].

The addition of Ca reduced the contents of different Cd chemical forms in *S. matsudana* (Fig. 6). The addition of Ca increased the percentage of 1 M NaCl-extracted Cd, but reduced the proportion of 0.6 M HCl- and 2% HAc-extracted Cd in *S. matsudana* leaves and roots compared to treatments with Cd alone, indicating that a larger proportion of Cd existed in the form of pectate- and protein-integrated Cd and non- or low-toxic complexes. A recent study also reported that the application of Ca may stimulate production of more peptides and proteins that can easily combine with Cd to alleviate Cd toxicity in plants [23]. However, more research needs to be conducted in this area.

Cd and Ca interactions

In this study, the addition of Ca decreased the uptake of Cd in *S. matsudana* roots by altering its adsorption mode. Ca application also promoted Cd transportation from roots to shoots and modified Cd subcellular localization and its chemical forms in both roots and leaves to alleviate Cd toxicity (Fig. 7). Based on the collective findings, it is likely that Ca and Cd compete at Cd adsorption sites in the soil as they possess similar chemical properties. When both Ca and Cd exist in the soil system, Ca reduces Cd uptake, thus reducing Cd toxicity in plants [19, 45]. Apart from reducing Cd uptake, exogenous Ca alleviated Cd toxicity in *S. matsudana* by decreasing the percentage of Cd in the cell wall of roots and leaves and increasing the percentage of Cd content in soluble fractions, suggesting that plants minimize Cd toxicity by combining the free Cd in the protoplasm to form metal complexes, which further fixed Cd in the vacuoles through vacuolar compartmentalization. Exogenous Ca alleviated the toxicity of Cd in *S. matsudana* as well by changing the percentage of Cd chemical forms of 2% HAc- and 0.6 M HCl-extracted Cd to 1 M NaCl-extracted Cd [23].

Additionally, Toyota et al. [76] found that glutamic acid, a stress and mechanical damage signaling substance, transformed the signal due to the increased Ca^{2+} concentrations in the cytoplasm, thus spreading the signal to distal organs and inducing defense responses. In this study, the addition of Ca increased Ca concentrations in the cytoplasm. Therefore, it is proposed that similar processes, also referred to by Toyota et al. [76], were initiated in *S. matsudana* and that Ca coordinated with Cd, which led to Cd subcellular redistribution and modified Cd chemical forms by changing the expression levels of transporters involved in Cd xylem loading and upward-translocation in both the roots and leaves.

Conclusions

In summary, exogenous Ca alleviated Cd physiological toxicity in *S. matsudana* under Cd stress and reduced Cd adsorption but increased translocation from the roots to shoots, thereby leading to the subcellular redistribution of Cd, increasing the proportion of Cd in soluble fractions, decreasing Cd in root

and leaf cell walls, and changing Cd chemical forms from 2% HAc- and 0.6 M HCl-extracted Cd to 1 M NaCl-extracted Cd. Moreover, after the addition of Ca, Cd was transferred through the root epidermis, cortex, endodermis, and vascular cylinder, transported to the shoots, and accumulated in leaf epidermal and mesophyll cells, but less so in leaf main veins and guard cells. These results suggested that the addition of Ca improved the phytoremediation of Cd contamination in this woody plant. In the future, *S. matsudana* could be used to phytoremediate areas that are severely contaminated with Cd where exogenous Ca can be moderately added to lighten the Cd toxic effects on the growth of willow trees and improve their survival rates, which is an economic way to detoxify woody plants.

Methods

Seedling cultivation and treatment

S. matsudana used in this experiment was identified and offered by Professor Wenhui Zhang of Northwest A&F University, China. The collection of the experimental materials conforms to the institutional, national or international guidelines. Woody cuttings (15 cm long) of 1-year-old *matsudana* shoots grown in the Science Park of Tianjin Normal University, China, were gathered and sprouted in plastic pots filled with tap water for 2 weeks under 23°C ± 5°C and 55% ± 10% relative humidity before experimentation. After the cuttings sprouted, healthy and orderly seedlings were cultivated in 1/2 Hogland nutrient solution for 28 d. Cd and Ca with different quantities were added to the culture solution to form five treatments: the control (without Cd or Ca), 10 μM Cd, 10 μM Cd + 5 mM Ca, 50 μM Cd, and 50 μM Cd + 5 mM Ca. The nutrient solution consisted of 5 mM KNO_3, 5 mM $Ca(NO_3)_2$, 1 mM KH_2PO_4, 50 μM H_3BO_3, 10 μM FeEDTA, 4.5 μM $MnCl_2$, 3.8 μM $ZnSO_4$, 0.3 μM $CuSO_4$, and 0.1 μM $(NH_4)_6Mo_7O_{24}$ adjusted to pH 5.5. Cadmium chloride ($CdCl_2 \times 2.5H_2O$) and Calcium chloride ($CaCl_2$) were used to supply Cd and Ca respectively. The culture solutions were changed every 7 d. An air pump was used during culturing.

Determination of Cd contents and TF calculation

Roots, old stem, new stem and leaves from each treatment were gathered separately after 28 d. The samples were washed thoroughly with running tap water and subsequently with deionized water. All the samples were dried in an oven at 45°C for 3 d, at 80°C for 1 d, and at 105°C for 12 h. After that, the samples were digested using wet-digestion methods. Cd contents were determined using inductively coupled plasma atomic emission spectrometry (ICP-AES) (Leeman Labs Inc., Mason, OH, USA). TF was calculated as Cd content in the aerial parts of plants ÷ total Cd content in the plant.

Measurement of chlorophyll fluorescence parameters

The chlorophyll fluorescence parameters quenching analysis was conducted at room temperature with a Dual-PAM/F portable fluorometer (Walz, Effeltrich, Germany). The plants of each treatment were darkened for 20 min prior to measurements. The fifth fully expanded leaf from the top shoot after 28 d was collected for measuring the chlorophyll fluorescence parameters with five replicates. F_0, F_m, F_v/F_m, Y(II), qP, qN, and other data were provided by the fluorometer.

Subcellular tissue separation by differential centrifugation

The 28-d-treated roots and leaves were cut and rinsed with deionized water. After absorbing the surface moisture, 3 g treated roots and leaves were accurately weighed, frozen, and homogenized in pre-cooled (4°C) extraction buffer (50 mM Tris-HCl, 250 mM sucrose, 1.0 mM $C_4H_{10}O_2S_2$, pH 7.5) with a chilled mortar and pestle [77]. Samples were divided into three parts (i.e., cell wall, cell organelles, and soluble fractions) following the methods reported by Xin et al. [78] and Wu et al. [25]. Cd concentrations in the three fractions were measured by an Analyst 400 atomic absorption spectrometer (PerkinElmer, Waltham, MA, USA).

Extraction of different Cd chemical forms

Different Cd chemical forms were successively extracted by designated solutions in the following order [25, 78]:

(1) 80% ethanol, Cd_E;

(2) deionized water, Cd_W;

(3) 1 M NaCl, Cd_{NaCl};

(4) 2% HAc, Cd_{HAc};

(5) 0.6 M HCl, Cd_{HCl};

(6) Cd in residues, Cd_R.

The extracted Cd by the above extracting solutions and residues were named Cd_E, Cd_W, Cd_{NaCl}, Cd_{HAc}, Cd_{HCl}, Cd_R respectively.

S. matsudana roots and leaves exposed to the five treatments after 28 d were collected, then rinsed with 20 mM EDTA and deionized water successively. Two-gram samples were accurately weighed, and 20 mL of the above extractants was added and homogenized for extraction. The homogenate was shaken at 25°C for 22 h, then centrifuged at 5000 rpm for 10 min. The supernatant liquid was poured off and stored, then 10 mL buffer solution was added and subsequently shaken at 25°C for 2 h, centrifuged at 5000 rpm for 10 min, and the supernatant liquid was combined and dried in an oven. The Cd content of supernatant liquid and residues had been digested by wet-digesting with HNO_3:$HClO_4$ (4:1, v/v), and determined by inductively coupled plasma atomic emission spectrometry (ICP-AES) (Leeman Labs Inc., Mason, OH, USA).

Scanning electron microscope observation and EDXA

The elemental composition and subcellular localization in freeze-dried leaf and root samples were investigated. Leaf samples were collected near the veins of *S. matsudana* stressed by 50 μM Cd and 50 μM Cd + 5 mM Ca after 28 d. Root samples were collected from the root tip mature areas of *S. matsudana* in Cd and Cd + Ca treatments for 24 h. Leaf and root samples were rapidly frozen in liquid nitrogen for 90 min. Frozen samples were immediately placed in an LGJ-10C lyophilizer (Karaltay Instruments Co., Ltd., Beijing, China) for 24 h. Cross-sections of the samples were coated with gold using an Emitech K550X sputter/coater (Quorum Group Ltd., London, England). Energy dispersive X-ray analysis was conducted using an FEI Nova NanoSEM 230 (FEI Company, Oregon, USA) appended with analysis Genesis Apollo 10 EDXA (FEI Company, Oregon, USA). The spectrum was collected at 30 keV for 80 s using an X-ray detector. The Cd composition in the samples was displayed as weight percent in relation to total elements (wt%).

Gene expression analysis by qRT-PCR

One hundred milligram *S. matsudana* root and leaf samples exposed to 50 μM Cd and 50 μM Cd + 5 mM Ca for 24 h were used for gene expression analysis. Total RNA was extracted using an easy-spin Plant RNA Extraction kit (Aidlab, Beijing, China). RNA concentrations were calculated basing on the optical density at 260 nm. First-Strand Synthesis SuperMix (TransScript, Beijing, China) was used for cDNA synthesis following the manufacturer's instructions. Every cDNA template was measured on a 7500 RT-PCR platform (Applied Biosystems, Foster City, CA, USA) using a SYBR Select Master mix (Applied Biosystems, Foster City, CA, USA). The program used for qRT-PCR was as follows: UDG activation at 50°C for 2 min, Amplitaq fast DNA polymerase, up-activation at 95°C for 2 min, 40 cycles of denaturation at 95°C or 15 s, and annealing/extension at 50°C for 1 min. The gene-specific forward and reverse primers and cDNA template were added to the SYBR Select Master mix. Primers for the genes were designed using Primer v5.0 (Primer-E Ltd., Plymouth, 2001) with gene sequences obtained from GenBank in the NCBI database. qRT-PCR experiments were conducted using two biological replicates with three technical replicates for each sample. Melting curves were used to assess amplification specificity. The relative quantities of the transcripts were analyzed using the comparative Ct method [79]. Nramp1, ZIP8, IRT1, HMA2, HMA4, and PCR1 primer sets are provided (Supplementary file: Table S1).

Statistical analyses

Data were visualized using SigmaPlot v12.5 (Systat Software Inc., San Jose, CA). Data are presented as the mean ± standard error (SE). Analyses were performed using SPSS v24.0 for Windows (SPSS Inc., Illinois, USA). For the equality of averages, Student's *t* test was conducted.

List Of Abbreviations

Cd, Ca, *S. matsudana*, HAC, HCl, NaCl, Cu, Fe, Zn, Mn, SEM, EDXA, CDF, HMA, NRAMP, ZIP, F_0, F_m, F_v/F_m, Y(II), qP, qN, Cd_E, Cd_W, Cd_{NaCl}, Cd_{HAc}, Cd_{HCl}, and Cd_R, ICP-AES, TF, PCR1

Declarations

Acknowledgments

We thank LetPub (www.letpub.com) for its linguistic assistance during the preparation of this manuscript.

Authors' contributions

XS participated in plant cultivation, experimental operation and collecting the materials. WX participated in the data analysis and helped draft the manuscript. YJ carried out materials collecting. JZ designed the study and drafted the manuscript. All authors have read and approved this manuscript.

Funding

This project was supported by Natural Science Foundation of China (grant No. 31901184) and Doctor Foundation of Tianjin Normal University (grant No. 52XB1914). The funding body supported the study, analysis of data and writing the manuscript.

Availability of data and materials

All data generated or analysed during this study are included in this published article [and its supplementary information files].

Ethics approval and consent to participate

Not applicable.

Consent for publication

Not applicable.

Competing interests

The authors declare that they have no competing interests.

References

1. Qu KC, Wang ZY, Tang KK, Zhu YS, Fan RF. Trehalose suppresses cadmium-activated Nrf2 signaling pathway to protect against spleen injury. Ecotox Environ Safe. 2019;181:224–
2. Zhang WL, Du Y, Zhai MM, Shang Q. Cadmium exposure and its health effects: a 19-year follow-up study of a polluted area in China. Sci Total Environ. 2014;470:224–8.
3. Goix S, Leveque T, Xiong TT, Schreck E, Baeza-Squiban A, Geret F, Uzu G, Austruy A, Dumat C. Environmental and health impacts of fine and ultrafine metallic particles: assessment of threat

scores. Environ Res. 2014;133:185–94.

4. Tomar PC, Lakra N, Mishra SN. Effect of cadaverine on *Brassica juncea* (L.) under multiple stress. Indian J Exp Biol. 2013;51(9):758–63.
5. Deng G, Li M, Li H, Yin LY, Li W. Exposure to cadmium causes declines in growth and photosynthesis in the endangered aquatic fern (*Ceratopteris pteridoides*). Aquat Bot. 2014;112:23–
6. Osmolovskaya NG, Dung VV, Kudryashova ZK, Kuchaeva LN, Popova NF. Effect of Cadmium on Distribution of Potassium, Calcium, Magnesium, and Oxalate Accumulation in *Amaranthus cruentus* Plants. Russ J Plant Physl. 2018;65(4): 553–62.
7. Shang XS, Xue WX, Jiang Y. Effects of Calcium on the Alleviation of Cadmium Toxicity in *Salix matsudana* and Its Effects on Other Minerals. Pol J Environ Stud. 2020;29(2):unpublished.
8. Wang Y, Wang XL, Wang Chao, Wang RJ, Peng F, Xiao X, Zeng J, Fan X, Kang HY, Sha LN, Zhang HQ, Zhou YH. Proteomic Profiling of the Interactions of Cd/Zn in the Roots of Dwarf Polish Wheat (*Triticum polonicum*) Front Plant Sci. 2016;7:1378.
9. Khan AR, Ulah I, Khan AL, Park GS, Waqas M, Hong SJ, Jung BK, Kwak Y, Lee IJ, Shin JH. Improvement in phytoremediation potential of Solanum nigrum under cadmium contamination through endophytic-assisted Serratia sp RSC-14 inoculation. Environ Sci Pollut Res. 2015;22(18):14032–
10. Luo ZB, He JL, Polle A, Rennenberg H. Heavy metal accumulation and signal transduction in herbaceous and woody plants: Paving the way for enhancing phytoremediation efficiency. Biotechnol Adv. 2016;34(6):1131–
11. Zhang W, Lin KF, Zhou J, Zhang W, Liu LL, Zhang QQ. Cadmium accumulation, subcellular distribution and chemical forms in rice seedling in the presence of sulfur. Environ Toxicol Phar. 2014;37(1):348–
12. Wan YS, Zhai J, Wang AW, Han H, Shen M, Wen X. Environmental Research on Remediation of Cd-contaminated Soil by Electrokinetic Remediation. 2019;28(107):873–81.
13. Huang DL, Gong XM, Liu YG, Zeng GM, Lai C, Bashir H, Zhou L, Wang DF, Xu PA, Cheng M, Wan J. Effects of calcium at toxic concentrations of cadmium in plants. Planta. 2017;245(5):863–
14. Nedjimi B. Can calcium protect Atriplex halimus subsp schweinfurthii against cadmium toxicity? Acta Botanica Gallica. 2009;156(3):391–
15. Marschner H. Mineral Nutrition of Higher Plants, 2nd Ed. Academic Press, San Diego, CA, USA. 1995.
16. Kiegle E, Gilliham M, Haseloff J, Tester M. Hyperpolarisation-activated calcium currents found only in cells from the elongation zone of *Arabidopsis thaliana* Plant J. 2000;21(2):225–9.
17. Zhou XH, Hao WM, Shi HF, Hou YZ, Xu QG. Calcium Homeostasis Disruption - a Bridge Connecting Cadmium-Induced Apoptosis, Autophagy and Tumorigenesis. Oncol Res Treat. 2015;38(6):311–
18. El-Beitagi HS, Mohamed HI. Alleviation of Cadmium Toxicity in *Pisum sativum* Seedlings by Calcium Chloride. Not Bot Horti Agrobo. 2013;41(1):157–68.

19. Hayat S, Ahmad A, Wani AS, Alyemeni MN, Ahmad A. Regulation of Growth and Photosynthetic Parameters by Salicylic Acid and Calcium in *Brassica juncea* under Cadmium Stress. Z Naturforsch C. 2014;69(11-12):452–8.
20. Hayakawa N, Tomioka R, Takenaka C. Effects of calcium on cadmium uptake and transport in the tree species *Gamblea innovans*. Soil Sci Plant Nutr. 2011;57(5):691–
21. Huang RZ, Jiang YB, Jia CH, Jiang SM, Yan XP. Subcellular distribution and chemical forms of cadmium in *Morus alba* Int J Phytoremediat. 2018;20(5):448–53.
22. Chen BC, Lai HY. Subcellular distribution of cadmium in two paddy rice varieties with different cooking Methods. Agric Sci. 2016;7(06):383–95.
23. Lu HP, Li ZA, Wu JT, Shen Y, Li YW, Zou B, Tang YT, Zhuang P. Influences of calcium silicate on chemical forms and subcellular distribution of cadmium in *Amaranthus hypochondriacus* Sci Rep. 2017;7:40583.
24. Shi G, Zhang Z, Liu C. Silicon influences cadmium translocation by altering subcellular distribution and chemical forms of cadmium in peanut roots. Arch Agron Soil Sci. 2017;63(1):117–23.
25. Wu HF, Wang JY, Li BB, Ou YJ, Wang JR, Shi QY, Jiang WS, Liu DH, Zou JH. *Salix matsudana* Koidz Tolerance Mechanisms to Cadmium: Uptake and Accumulation, Subcellular Distribution, and Chemical Forms. Pol J Environ Stud. 2016a;25(4):1739–
26. Xu PX, Wang ZL. Physiological mechanism of hypertolerance of cadmium in Kentucky bluegrass and tall fescue: chemical forms and tissue distribution. Environ Exp Bot. 2013;96(35-42):35–42.
27. Luo N, Li X, Chen AY, Zhang LJ, Zhao HM, Xiang L, Cai QY, Mo CH, Wong MH, Li H. Does arbuscular mycorrhizal fungus affect cadmium uptake and chemical forms in rice at different growth stages? Sci Total Environ. 2017;599–600:1564–
28. Yin AG, Yang ZY, Ebbs S, Yuan JG, Wang JB, Yang JZ. Effects of phosphorus on chemical forms of Cd in plantsof four spinach (*Spinacia oleracea*) cultivars differing in Cd accumulation. Environ Sci Pollut Res. 2016;23(6):5753–62.
29. Wu HF, Wang JY, Ou YJ, Li BB, Jiang WS, Liu DH, Zou JH. Cadmium uptake and localization in roots of *Salix matsudana* Fresen Environ Bull. 2016b;25(7): 2700–6.
30. Shi QY, Wang JR, Zou JH, Jiang Z, Wang JY, Wu HF, Jiang WS, Liu DH. Cadmium uptake and accumulation and its toxic effects on leaves in *Hordeum vulgare*. Fresen Environ Bull. 2015;24(12A):4504–
31. Liu DH, Kottke I, Adam D. Localization of cadmium in the root cells of *Allium cepa* by energy dispersive X-ray analysis. Biol Plant. 2007;51(2):363–6.
32. Jiao YQ, Ge W, Qin R, Sun BL, Jiang WS, Liu DH. Influence of cadmium stress on growth, ultrastructure and antioxidative enzymes in Populus 2025. Fresenius Environ Bull. 2012;21(6):1375–
33. Ge W, Jiao YQ, Zou JH, Jiang WS, Liu DH. Ultrastructural and photosysthetic response of *Populus* 107 leaves to cadmium stress. Pol J Environ Stud. 2015;24(2):519–27.

34. Kim YH, Khan AL, Kim DH, Lee SY, Kim KM, Waqas M, Jung HY, Shin JH, Kim JG, Lee IJ. Silicon mitigates heavy metal stress by regulating P-type heavy metal ATPases, Oryza sativalow silicon genes, and endogenous phytohormones. BMC Plant Biol. 2014;14(1):13.
35. Fan W, Liu CY, Cao BN, Qin ML, Long DP, Xiang ZH, Zhao AC. Genome-Wide Identification and Characterization of Four Gene Families Putatively Involved in Cadmium Uptake, Translocation and Sequestration in *Mulberry*. Front Plant Sci. 2018;9:879.
36. Chanroj S, Wang GY, Venema K, Zhang MW, Delwiche CF, Sze H. Conserved and diversified gene families of monovalent cation/H^+ antiporters from algae to flowering plants. Front Plant Sci. 2012;3:1–
37. Li BB, Ouyang J, Li CH, Shang XS, Zou JH. Response to NaCl Stress in *Salix matsudana* Koidz Seedlings. Pol J Environ Stud. 2018;27(2):753–
38. Yang JX, Li XL, Hu YB, Gao LM, Yao DX. Enrichment Characteristics of heavy metal cadmium in woody plants system. Kem Ind. 2015;64(5-6):283–
39. Zou JH, Wang G, Ji J, Wang JY, Wu HF, Ouyang J, Li BB. Transcriptional, physiological and cytological analysis validated the roles of some key genes linked Cd stress in *Salix matsudana* Environ Exp Bot. 2017;134:116–29.
40. Perveen A, Wahid A, Javed F. Varietal Differences in Spring and Autumn Sown Maize (Zea mays) for Tolerance against Cadmium Toxicity. Int J Agric Biol. 2011;13(6):909–
41. Gao ML, Yang YJ, Song ZG. Effects of graphene oxide on cadmium uptake and photosynthesis performance in wheat seedlings. Ecotox Environ Safe. 2019;173:165–73.
42. He LZ, Yu L, Li B, Du NS, Guo SR. The effect of exogenous calcium on cucumber fruit quality, photosynthesis, chlorophyll fluorescence, and fast chlorophyll fluorescence during the fruiting period under hypoxic stress. Bmc Plant Biology. 2018;18:18.
43. Qi HY, Wang D, Qi MF, Liu YF, He Y, Li TL. Regulation of different calcium forms on the photosynthesis of tomato leaves under heat stress. The Journal of Applied Ecology. 2014;25(12):3540–
44. Shi QY, Wang JR, Zou JH, Jiang Z, Wang JY, Wu HF, Jiang WS, Liu DH. Cd Subcellular Localization in Root Tips of *Hordeum vulgare*. Pol J Environ Stud. 2016;25(2):903–
45. Zeng LH, Zhu T, Gao Y, Wang YT, Ning CJ, Björna LO, Chen D, Li SS. Effects of Ca addition on the uptake, translocation, and distribution of Cd in *Arabidopsis thaliana*. Ecotox Environ Safe. 2017;139:228–37.
46. Nakanishi H, Ogawa I, Ishimaru Y, Mori S, Nishizawa NK. Iron deficiency enhances cadmium uptake and translocation mediated by the Fe^{2+} transporters OsIRT1 and OsIRT2 in rice. Soil Sci Plant Nutr. 2006;52(4):464–9.
47. Kurtyka R, Małkowski E, Kita A, Karcz W. Effect of calcium and cadmium on growth and accumulation of cadmium, calcium, potassium and sodium in maize seedlings. Pol J Environ Stud. 2008;17(1):51–6.

48. Wang CQ, Song H. Calcium protects *Trifolium repens* seedlings against cadmium stress. Plant Cell Rep. 2009;28(9):1341–9.
49. Wang CY, Wang SJ, Rong L, Luo XQ. Analyzing about characteristics of calcium content and mechanisms of high calcium adaptation of common pteridophyte in Maolan karst area of China. Chin. J Plant Ecol. 2011;35:1061–9.
50. Talukdar Exogenous calcium alleviates the impact of cadmium-induced oxidative stress in *Lens culinaris* Medic. Seedlings through modulation of antioxidant enzyme activities. J Crop Sci Biotechnol. 2012;15(4):325–34.
51. Farzadfar S, Zarinkamar F, Modarres-Sanavy S, Hojati M. Exogenously applied calcium alleviates cadmium toxicity in *Matricaria chamomilla* plants. Environ Sci Pollut Res. 2013;20(3):1413–22.
52. Gong XM, Liu YG, Huang DL, Zeng GM, Liu SB, Tang H, Zhou L, Hu X, Zhou YY, Tan XF. Effects of exogenous calcium and spermidine on cadmium stress moderation and metal accumulation in *Boehmeria nivea* (L.) Gaudich. Environ Sci Pollut Res. 2016;23(9):8699–708.
53. Mills RF, Francini A, da Rocha PSCF, Baccarini PJ, Aylett M, Krijger GC, Williams LE. The plant P1B-type ATPase AtHMA4 transports Zn and Cd and plays a role in detoxification of transition metals supplied at elevated levels. FEBS Lett. 2005;579(3):783–91.
54. Mills RF, Peaston KA, Runions J, Williams LE. HvHMA2, a P1B-ATPase from barley, is highly conserved among cereals and functions in Zn and Cd transport. Plos One. 2012;7(8):e42640.
55. Song WY, Martinoia E, Lee J, Kim D, Kim DY, Vogt E, Shim D, Choi KS, Hwang I, Lee Y. A novel family of cys-rich membrane proteins mediates cadmium resistance in *Arabidopsis*. Plant Physiol. 2004;135(2):1027–39.
56. Song WY, Choi KS, Alexis DA, Martinoia E, Lee Y. Brassica juncea plant cadmium resistance 1 protein (BjPCR1) facilitates the radial transport of calcium in the root. Proc Natl Acad Sci USA. 2011;108(49):19808–13.
57. Karley AJ, Leigh RA, Sanders D. Where do all the ions go? The cellular basis of differential ion accumulation in leaf cells. Trends Plant Sci. 2000;5(11):465–70.
58. Huguet S, Bert V, Laboudigue A, Barthes V, Lsaure MP, Llorens I, Schat H, Sarrt G. Cd speciation and localization in the hyperaccumulator Arabidopsis halleri. Environ Exp Bot. 2012;82:54–
59. Leitenmaier B, Kupper H. Cadmium uptake and sequestration kinetics in individual leaf cell protoplasts of the Cd/Zn hyperaccumulator Thlaspi caerulescens. Plant Cell Environ. 2011;34(2):208–
60. Xin JL, Huang BF. Subcellular Distribution and Chemical Forms of Cadmium in Two Hot Pepper Cultivars Differing in Cadmium Accumulation. J Agric Food Chem. 2019;62(2):508–
61. Xin JL, Huang BF, Yang ZY, Yuan JG, Zhang YD. Comparison of cadmium subcellular distribution in different organs of two water spinach (*Ipomoea aquatica*) cultivars. Plant Soil. 2013;372(1-2):431–44.
62. Li GX, Li QS, Wang L, Chen GY, Zhang DD. Subcellular distribution, chemical forms, and physiological response to cadmium stress in *Hydrilla verticillata.* J. Phytoremediat. 2019;21(3):230–9.

63. Saraswat S, Rai JPN. Complexation and detoxification of Zn and Cd in metal accumulating plants. Rev Environ Sci Bio-Technol. 2011;10(4):327–
64. Ouyang J, Li BB, Xue WX, Jiang Y, Li CH, Shang XS, Zou JH. Cadmium uptake and accumulation, subcellular distribution and chemical forms in young seedlings of *Salix babylonica* Fresenius Environ Bull. 2019;28(5):3637–48.
65. Wang JB, Su LY, Yang JZ, Yuan JG, Yin AG, Qiu Q, Zhang K, Yang ZY. Comparisons of cadmium subcellular distribution and chemical forms between low-Cd and high-Cd accumulation genotypes of watercress (*Nasturtium officinale* R. Br.) Plant Soil. 2015;396(1-2):325–37.
66. Ma JF, Ueno D, Zhao FJ, McGrath SP. Subcellular localisation of Cd and Zn in the leaves of a Cd-hyperaccumulating ecotype of *Thlaspi caerulescens.* 2005;220(5):731–6.
67. Choi YE, Harada E, Wada M, Tsuboi H, Morita Y, Kusano T, Sano H. Detoxification of cadmium in tobacco plants: formation and active excretion of crystals containing cadmium and calcium through trichomes. Planta. 2001;213(1):45–
68. Lai HY, Cai MC. Effects of extended growth periods on subcellular distribution, chemical forms, and the translocation of cadmium in Impatiens Walleriana. Intern J Phytorem. 2016;18(3):228–34.
69. Wang ST, Dong Q, Wang ZL. Differential effects of citric acid on cadmium uptake and accumulation between tall fescue and Kentucky bluegrass. Ecotox Environ Safe. 2017;145:200–
70. Zhang C, Zhang P, Mo C, Yang W, Li Q, Pan L, Lee DK. Cadmium uptake, chemical forms, subcellular distribution, and accumulation in *Echinodorus osiris* Environ Sci Process Impacts. 2013;15(7):1459–65.
71. Yang WD, Chen YT, Qu MH. Subcellular distribution and chemical forms of cadmium in *Salix matsudana*. Acta Bot Boreal-Occident Sin. 2009;29:1394–
72. Zhang XF, Zhang XH, Gao B, Li ZA, Xia HP, Li HF, Li J. Effect of cadmium on growth, photosynthesis, mineral nutrition and metal accumulation of an energy crop, king grass (*Pennisetum americanum* × P. purpureum). Biomass Bioenerg. 2014;67:179–
73. Weng BS, Xie XY, Weiss DJ, Liu JC, Lu HL, Yan CL. Kandelia obovata (S., L.) Yong tolerance mechanisms to cadmium: sub-cellular distribution, chemical forms and thiol pools. Mar Pollut Bull. 2012;64(11):2453–
74. Li XD, Ma H, Li LL, Gao YF, Li YZ, Xu H. Subcellular distribution, chemical forms and physiological responses involved in cadmium tolerance and detoxification in *Agrocybe Aegerita*. Ecotox Environ Safe. 2019;171:66–
75. Qiu Q, Wang YT, Yang ZY, Yuan JG. Effects of phosphorus supplied in soil on subcellular distribution and chemical forms of cadmium in two Chinese flowering cabbage (*Brassica parachinensis*) cultivars differing in cadmium accumulation. Food Chem Toxi. 2011;49(9):2260–7.
76. Toyota M, Spencer D, Sawai-Toyota S, Wng JQ, Zhang T, Koo AJ, Howe GA, Gilroy S. Glutamate triggers long-distance, calcium-based plant defense signaling. Science. 2018;361(6407):1112–
77. Weigel HJ, Jager HJ. Subcellular distribution and chemical form of cadmium in bean plants. Plant Physiol. 1980;65(3):480–

78. Xin J, Huang B, Dai H, Liu A, Zhou W, Liao K. Characterization of cadmium uptake, translocation, and distribution in young seedlings of two hot pepper cultivars that differ in fruit cadmium concentration. Environ Sci Pollut Res. 2014;21(12):7449–56.

79. Livak KJ, Schmittgen TD. Analysis of relative gene expression data using real-time quantitative PCR and the 2 (-Delta Delta C(T)) method. Methods. 2001;25(4):402–

Tables

Table 1. Effects of Cd and Cd + Ca on *S. matsudana* photosynthetic fluorescence parameters.

Parameter	Treatment Cd (μmol/L) Ca (mmol/L)				
	0	10 Cd	10 Cd + 5 Ca	50 Cd	50 Cd + 5 Ca
F_0	0.07 ± 0.01a	0.07 ± 0.01b	0.07 ± 0.01ab	0.06 ± 0.01c	0.07 ± 0.01b
F_m	0.40 ± 0.01a	0.36 ± 0.03b	0.37 ± 0.01c	0.32 ± 0.01d	0.36 ± 0.01e
F_v/F_m	0.81 ± 0.01a	0.80 ± 0.02b	0.81 ± 0.03c	0.79 ± 0.02d	0.80 ± 0.02bc
Y (II)	0.64 ± 0.02a	0.62 ± 0.01b	0.63 ± 0.01c	0.59 ± 0.01d	0.61 ± 0.01e
qP	0.87 ± 0.01a	0.81 ± 0.01b	0.82 ± 0.01c	0.80 ± 0.01d	0.81 ± 0.01e
qN	0.23 ± 0.01a	0.25 ± 0.02b	0.24 ± 0.01c	0.30 ± 0.01d	0.27 ± 0.01

Different lower-case letters represent significant differences ($p < 0.05$, *t* test). Data are presented as the mean ± SE (n = 6).

Table 2. Effects of Ca addition on Cd contents in different organs and TFs in *S. matsudana* .

Treatment Cd (μmol/L) Ca (mmol/L)	Cd (μg/g, DW ± SE)				TF (%)
	Root	New stem	Leaf	Old stem	
0	5.89 ± 0.01a	5.81 ± 0.01a	7.11 ± 0.00a	1.48 ± 0.07a	
10 Cd	1365.40 ± 0.44b	105.46 ± 1.75b	174.93 ± 0.21b	28.04 ± 0.01b	18.42
10 Cd + 5 Ca	1207.20 ± 0.22c	97.83 ± 0.08c	164.68 ± 2.29c	20.90 ± 1.22c	19.01
50 Cd	3422.11 ± 3.59d	223.00 ± 0.57d	188.24 ± 1.44d	56.74 ± 0.08d	12.03
50 Cd + 5 Ca	3014.00 ± 1.17e	206.89 ± 0.42e	176.54 ± 0.57e	51.53 ± 1.08e	12.61

Different lower-case letters represent significant differences ($p < 0.05$, *t* test). Data are presented as the mean ± SE (n = 3).

Table 3. Cd content in the subcellular components (μg/g FW) of *S. matsudana* roots and leaves exposed to different Cd and Cd + Ca concentrations for 28 d.

Organ	Treatment Cd (μmol/L) Ca (mmol/L)	Fresh weight (μg·g⁻¹) ± SE		
		Cell wall	Cell organelle	Soluble fraction
Leaves	10 Cd	7.912 ± 0.012a	2.372 ± 0.003a	9.297 ± 0.031a
	10 Cd + 5 Ca	4.786 ± 0.012b	1.493 ± 0.015b	6.590 ± 0.015b
	50 Cd	9.761 ± 0.009c	3.111 ± 0.039c	10.725 ± 0.008c
	50 Cd +5 Ca	4.764 ± 0.028b	1.872 ± 0.015d	8.339 ± 0.031d
Roots	10 Cd	76.167 ± 0.003a	4.636 ± 0.016a	28.731 ± 0.027a
	10 Cd + 5 Ca	62.361 ± 0.024b	3.981 ± 0.013b	26.769 ± 0.034b
	50 Cd	319.641 ± 0.019c	11.342 ± 0.017c	82.964 ± 0.033c
	50 Cd + 5 Ca	265.650 ± 0.018d	7.636 ± 0.014d	76.789 ± 0.013d

Different lower-case letters represent significant differences ($p < 0.05$, *t* test). Data are presented as the mean ± SE (n = 3).

Table 4. Cd contents of different Cd chemical forms in *S. matsudana* stressed by Cd and Cd + Ca for 28 d.

Organ	Treatment Cd (μmol/L) Ca (mmol/L)	Fresh weight (μg·g⁻¹) ± SE					
		Cd_E	Cd_W	Cd_{NaCl}	Cd_{HAc}	Cd_{HCl}	Cd_R
Roots	10 Cd	3.367 ± 0.015a	7.26 ± 0.022a	41.461 ± 0.033a	36.183 ± 0.018a	16.11 ± 0.054a	1.217 ± 0.015a
	10 Cd + 5 Ca	2.023 ± 0.014b	9.67 ± 0.014b	44.08 ± 0.022b	30.57 ± 0.012b	8.95 ± 0.018b	1.042 ± 0.018b
	50 Cd	9.161 ± 0.014c	12.74 ± 0.021c	117.937 ± 0.025c	111.927 ± 0.028c	61.16 ± 0.025c	3.133 ± 0.029c
	50 Cd + 5 Ca	3.829 ± 0.027d	27.15 ± 0.025d	118.80 ± 0.016d	83.96 ± 0.026d	35.40 ± 0.037d	2.329 ± 0.022d
Leaves	10 Cd	0.85 ± 0.021a	2.46 ± 0.007a	14.10 ± 0.025a	7.96 ± 0.011a	3.25 ± 0.007a	0.58 ± 0.015a
	10 Cd + 5 Ca	0.59 ± 0.024b	2.20 ± 0.011b	12.01 ± 0.019b	5.58 ± 0.017b	2.17 ± 0.015b	0.44 ± 0.011b
	50 Cd	1.45 ± 0.021c	1.98 ± 0.012c	14.92 ± 0.013c	12.37 ± 0.014c	4.55 ± 0.013c	0.70 ± 0.012c
	50 Cd + 5 Ca	0.98 ± 0.013d	2.10 ± 0.011d	15.83 ± 0.015d	7.10 ± 0.026d	3.62 ± 0.013d	0.61 ± 0.019d

Different lower-case letters represent significant differences ($p < 0.05$, t test). Data are presented as the mean ± SE (n = 3).

Additional File

Additional file: Table S1. Sequences of qRT-PCR primers.

Figures

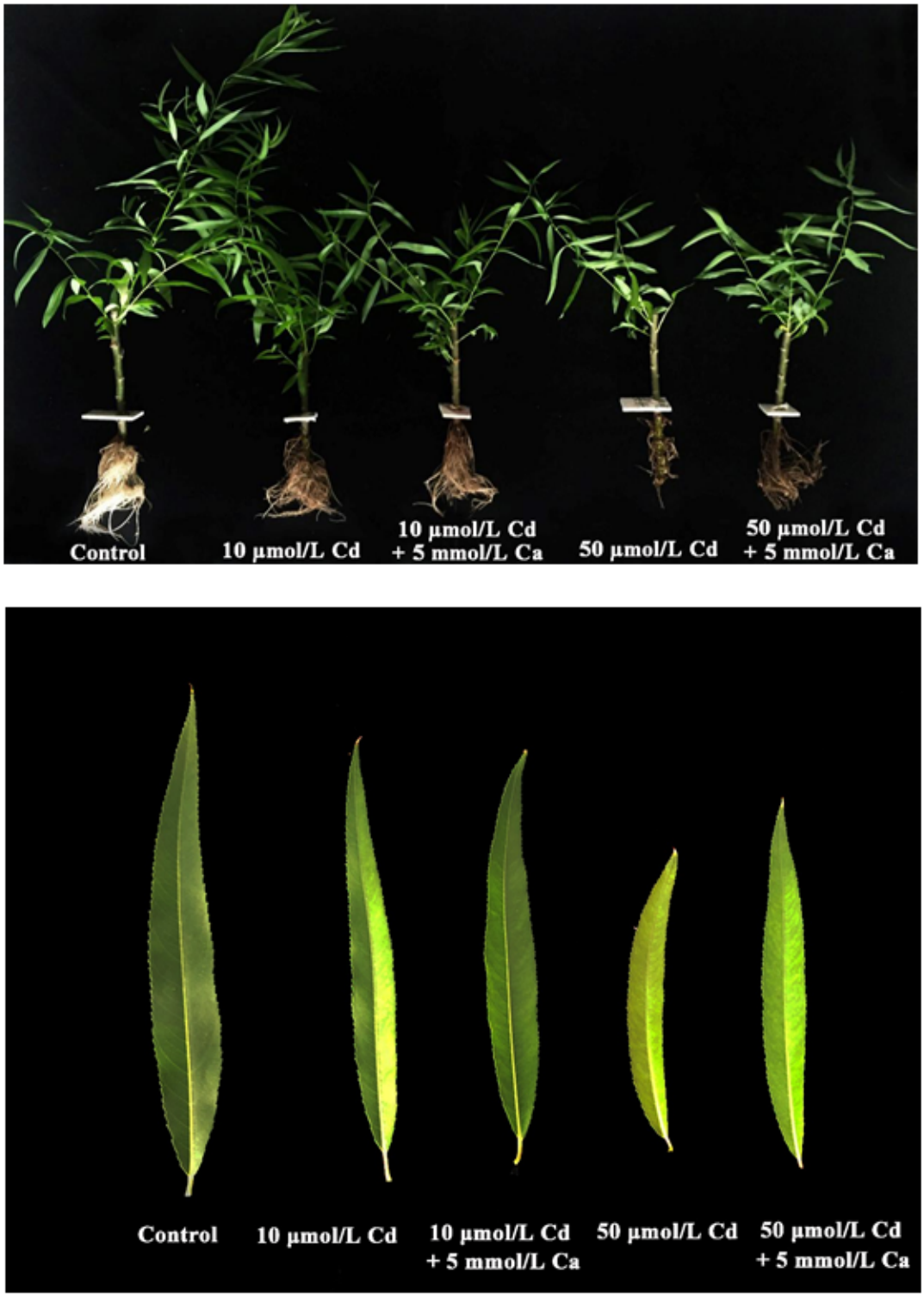

Figure 1

Effects of Cd and Cd + Ca concentrations on S. matsudana plant growth and leaf morphology after 28 d.

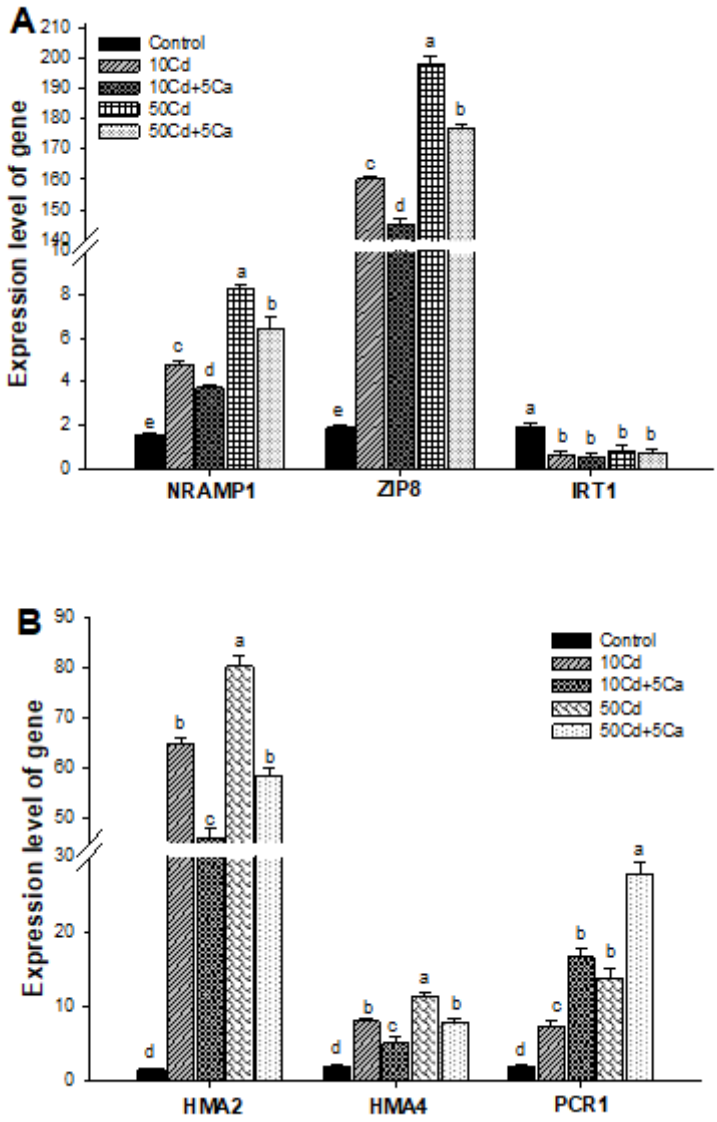

Figure 2

qRT-PCR analysis of the genes involved in Cd uptake and xylem loading, including NRAMP1, ZIP8, IRT1, HMA2, and HMA4, as well as PCR1, the gene involved in Ca transport. Data are presented as the mean ± SE (n = 3).

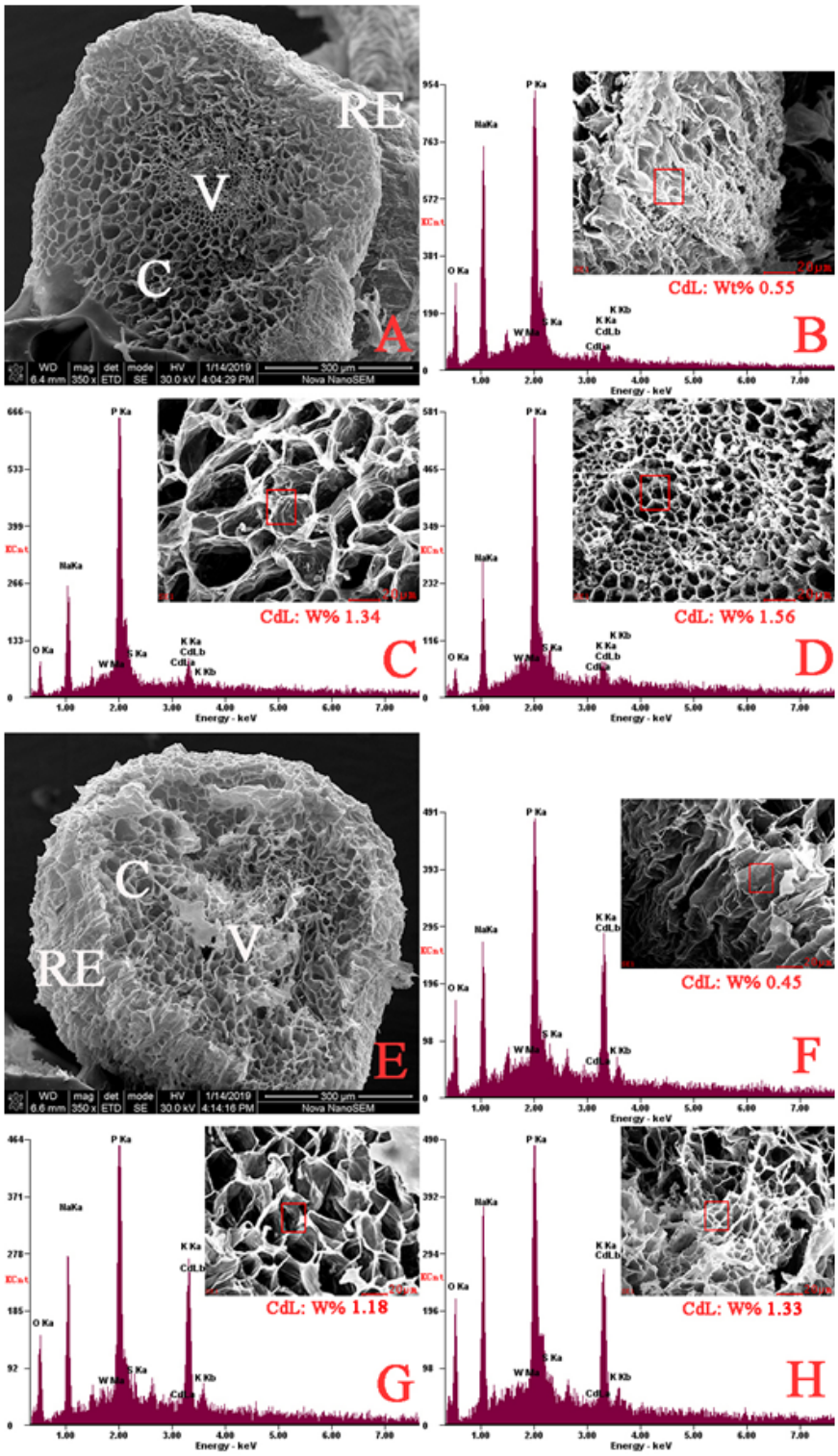

Figure 3

SEM micrographs and Cd localization in S. matsudana roots exposed to 50 μmol/L Cd (A–D) and 50 μmol/L Cd + 5 mmol/L Ca (E–H) for 28 d. A, E: Transverse section of root tip mature area (scale bars = 300 μm); B, F: Root epidermal cells (scale bars = 20 μm); C, G: Root cortex cells (scale bars = 20 μm); D, H: Root vascular column cells (scale bars = 20 μm). Red box sites of the analysis; x-axis-energy [keV]. RE = Root epidermis; C = Cortex; V = Vascular cylinder.

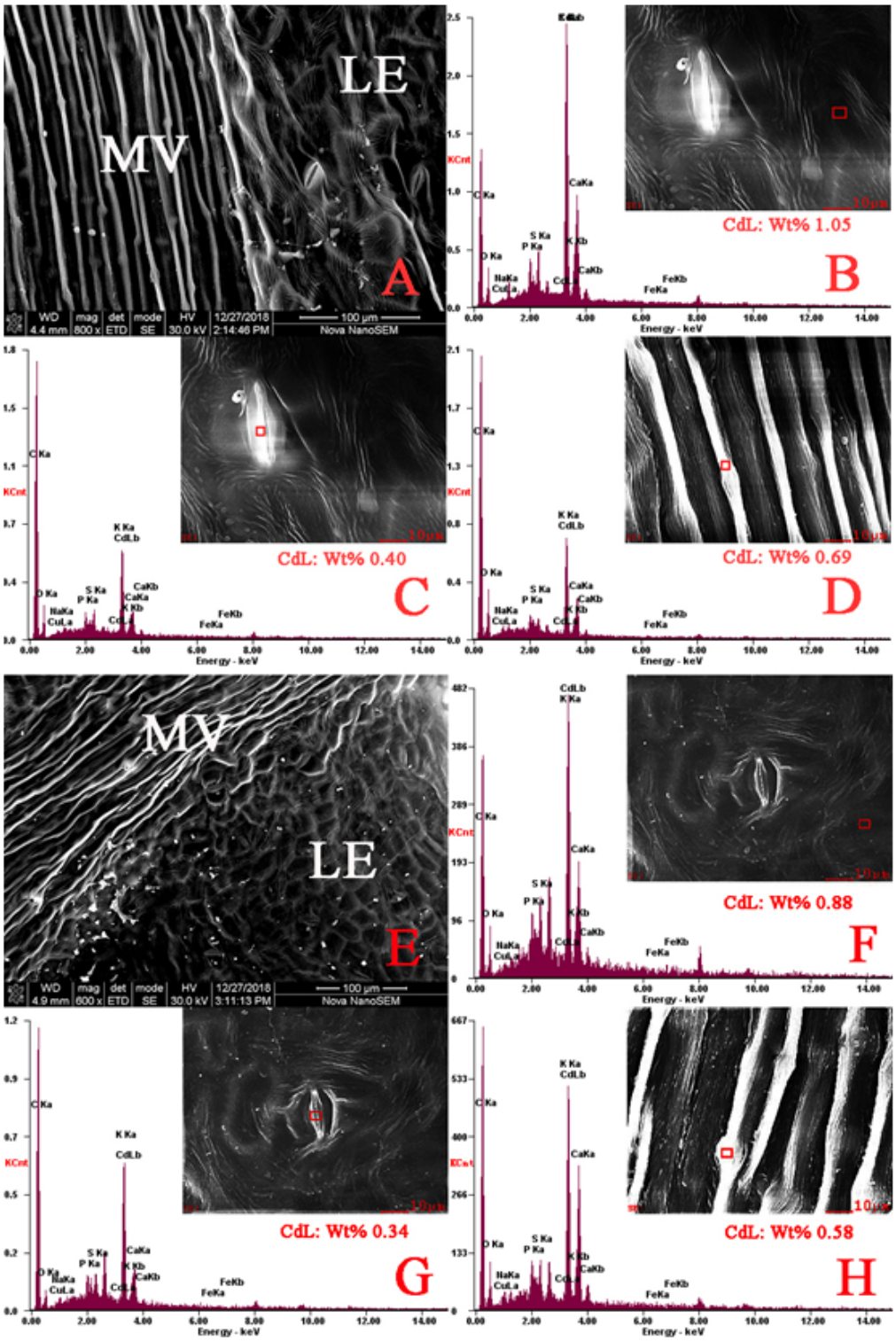

Figure 4

SEM micrographs and Cd localization in S. matsudana leaves exposed to 50 μmol/L Cd (A–D) and 50 μmol/L Cd + 5 mmol/L Ca (E–H) for 28 d. A, E: Transverse section of a leaf (scale bars = 100 μm); B, F: Leaf epidermal cells (scale bars = 10 μm); C, G: Leaf epidermal stomata (scale bars = 10 μm); D, H: Leaf main vein (scale bars = 10 μm). Red box sites of the analysis; x-axis-energy [keV]. LE = leaf epidermis; MV = main vein.

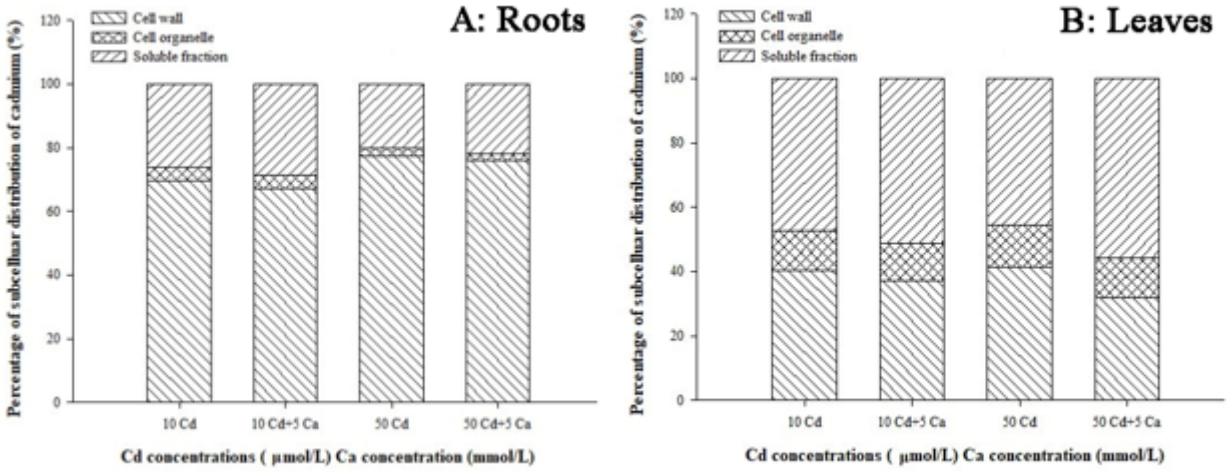

Figure 5

Percentage of Cd contents in different subcellular fractions of S. matsudana exposed to Cd and Cd + Ca for 28 d. A: Roots; B: Leaves.

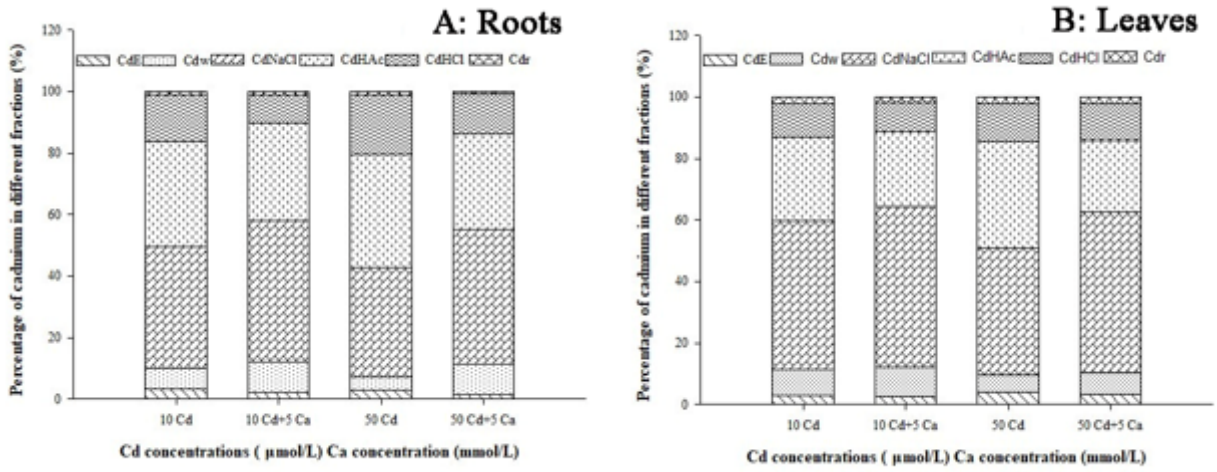

Figure 6

Proportions of different Cd chemical forms in S. matsudana exposed to Cd and Cd + Ca for 28 d. A: Roots; B: Leaves.

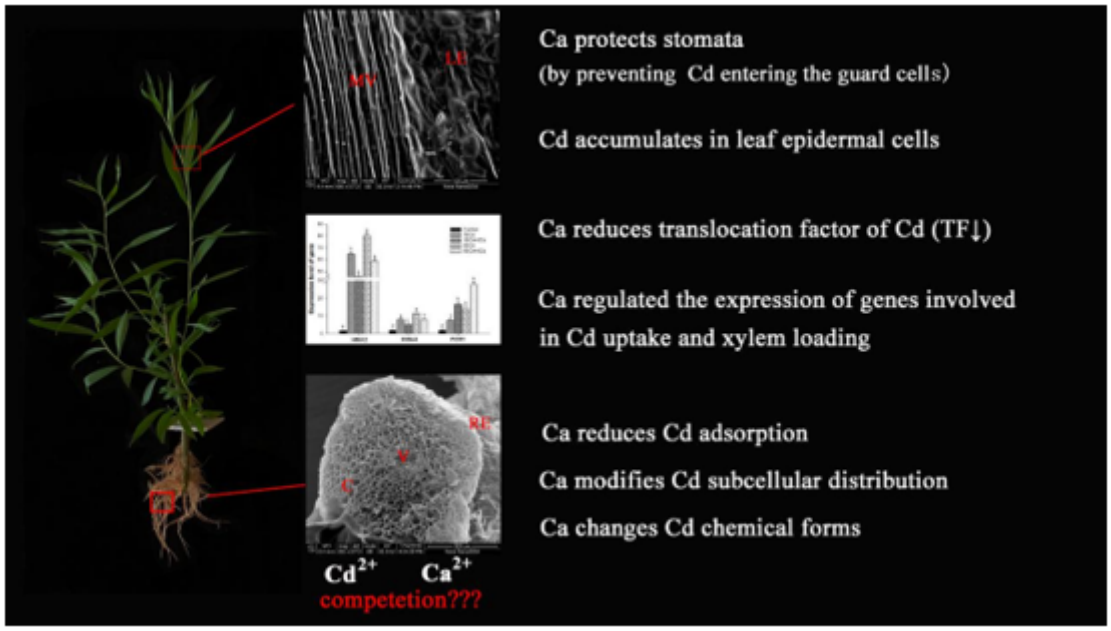

Figure 7

Schematic diagram of Ca alleviating Cd-induced toxicity in S. matsudana.

Supplementary Files

This is a list of supplementary files associated with this preprint. Click to download.

- Supplementaryfile.docx